Pairing effects on vorticity of incident neutron currents at quasiparticle resonance energies in *n-A* elastic scattering

K. Mizuyama [1,2] H. Dai Nghia [3,4] T. Dieu Thuy,[3] N. Hoang Tung [5] and T. V. Nhan Hao [3,4,*]

[1]*Institute of Research and Development, Duy Tan University, Da Nang 550000, Vietnam*
[2]*Faculty of Natural Sciences, Duy Tan University, Da Nang 550000, Vietnam*
[3]*Faculty of Physics, University of Education, Hue University, 34 Le Loi Street, Hue City 49000, Vietnam*
[4]*Center for Theoretical and Computational Physics, University of Education, Hue University, 34 Le Loi Street, Hue City 49000, Vietnam*
[5]*Faculty of Physics, The University of Danang, University of Science and Education, Da Nang 550000, Vietnam*

In this study, we analyzed how the incident neutron current is affected by the pairing effect in neutron-nucleus scattering described within the framework of Hartree-Fock-Bogoliubov theory by performing numerical calculations in terms of current, vorticity, and circulation of the incident neutron current. We found that the pairing effect on the incident neutron flux is completely different between particle-type and hole-type quasiparticle resonances. In the case of h-type quasiparticle resonance, the pairing acts to prevent the neutron flux from entering the nucleus, reducing circulation. In the case of p-type quasiparticle resonance, pairing acts to reduce circulation at energies lower than the resonance energy, but, at energies higher than the resonance energy, the effect of pairing on the neutron flux is reversed and, conversely, circulation is increased. These properties are consistent with the approximate expression for the vorticity characteristics at p-type and h-type resonances, implying that the vorticity appearing near p-type resonances due to the pair-correlation effect is inversely proportional to the resonance width (proportional to the resonance lifetime). In contrast, at h-type resonances, the pair-correlation effect has the effect of canceling out the vortex created by MF scattering and is independent of the resonance width.

I. INTRODUCTION

Quantum vortices have been introduced as quantized circulation in superfluids and magnetic flux in superconductors to understand the properties of superfluid helium, type II superconductors, Bose-Einstein condensation of ultracold atoms, etc. [1–6], and have been successfully observed experimentally [7]. Superfluid phase transition is thought to be caused by the excitation of quantum vortices. Also in nuclear physics, the coupling rotation of the deformed nucleus and the intrinsic vorticity has been discussed as the superfluidity phenomena [8–10]. The effect of superfluid vortices in the interior of neutron stars has also been discussed [11–14].

Even if we consider it apart from the nature of superfluidity, a vortex is a phenomenon that is easy to imagine intuitively and is very characteristic in physics in general, as seen in typhoons and tornadoes. In nuclear physics, vortex motion has often been proposed as one of the characteristic collective modes of nuclei (toroidal mode) [15,16]. This is because vortex motion has a unique topological structure and dynamic stability (as seen in Kelvin's circulation theorem, etc.), and can appear anywhere in a system where there is a current.

In neutron-nucleus (*n-A*) scattering, resonances are observed as sharp peaks with small widths at all cross

sections given as a function of incident neutron energy. It is known that the cross section satisfies the optical theorem when there is no absorption effect on the potential in the fundamental equations (such as the Schrödinger equation, the Hartree-Fock-Bogoliubov equation, and so on), which means that the neutron flux current satisfies the continuity equation, i.e., the current is conserved. According to Helmholtz's theorem, the current can be divided into the current with vortices and the current without vortices. Regardless of the conservation laws of the current, vortices can generally always be present in the current, unless the wave function (as the solution used to define the current) is constrained to be vortex free, or the system requires a vortex-free condition [17].

Given the stability of vortices due to their special topological properties and the metastable fundamental characteristic of resonance, the existence and the contribution of vortices to the resonant state can be expected. The vortices (vortexlike current) that can appear in the neutron flux of *n-A* scattering may be different from what has been defined as a quantum vortex (whose circulation can be quantized), but may characterize the resonances in the *n-A* scattering system.

Within the framework of Hartree-Fock-Bogoliubov (HFB) theory, the resonances appearing in *n-A* scattering include shape resonances formed by centrifugal barriers and quasiparticle resonances formed by pair-correlation effects. There are two types of quasiparticle resonances: particle (p) and hole (h) type quasiparticle resonances [18–21]. In [20,21], we

---

*Corresponding author: tvnhao@hueuni.edu.vn

discussed the formation conditions of the resonances appearing in *n-A* scattering and the effects of pair correlation in terms of the *S*- and *K*-matrix poles.

In terms of resonance energy and width, our previous results in [20,21] are qualitatively consistent with the results in [22] when the mean pair gap is given within the ordinary range. In other words, the pair-correlation effect is negligibly small for wide width resonances, which we classified as "shape resonances" in [21]. And the continuum effect caused by the pair-correlation effect on quasiparticle resonances due to the p-h configuration mixing is negligibly small.

However, we have also identified other properties of quasiparticle resonances caused by continuum effects (metastable structure of the wave function of h-type resonances, correlations between *K*- and *S*-matrix poles, and the Fano effect [23]).

The metastable structure of the h-type resonance is created by the coupling of the wave function of the bound hole state with the continuum through p-h configuration mixing by pair correlation. The correlation between the poles of the *K* matrix and the poles of the *S* matrix is a correlation caused by pair correlation, which gives rise to the disappearance of the metastable structure of the resonant wave function and the effect of vanishing *K*-matrix poles. The Fano effect is a continuum effect that occurs under special conditions for resonance states. When this effect occurs, the existence condition of resonance (simultaneous presence of *K*- and *S*-matrix poles) does not disappear, but the metastable structure of the wave function is lost, which appears as a characteristic shape in the nucleon-nucleus scattering cross section.

These results suggest that the continuum effect in quasiparticle resonance is more evident in the behavior of other phenomena and physical quantities than in the resonance energy or width. The neutron current in *n-A* scattering is a complex combination of various partial wave components of a continuum. Therefore, in order to investigate the unknown characteristic of quasiparticle resonance, in this paper we focus on the neutron current and the vortex it creates.

In *n-A* scattering, it is realistic to use complex optical potentials with absorption effects to quantitatively reproduce experimental values. However, according to Feshbach's theory, the origin of the complex optical potential is channel coupling, but at the same time channel coupling can be also the origin of sharp resonances. In [24], the continuum particle-vibration coupling (cPVC) method based on the Skyrme effective two-body interaction was applied to *n-A* scattering, and it was found that the complex optical potential calculated by the cPVC method not only quantitatively reproduces the cross sections, but also reproduces some of the sharp resonance structure. Those sharp resonances are caused by the coupling of incident neutrons with the excited states (RPA states) of the target nucleus, especially with giant resonances. This is consistent with Feshbach's theory, and the same may occur when the target nucleus is an open shell nucleus, i.e., sharp resonances may appear due to the coupling between the incident neutrons as quasiparticle states and the QRPA states of the target nucleus. In reality, the quasiparticle resonance observed experimentally in *n-A* scattering is likely to be caused by such a mechanism. However, a continuum quasiparticle-vibration coupling (cQVC) method, which takes pair correlation into account in the cPVC method, is required to analyze such quasiparticle resonances, but no one has achieved it yet. Furthermore, the characteristic of the quasiparticle resonances that emerges within the framework of HFB theory as the zeroth-order approximation has not yet been fully clarified. Existing phenomenological complex optical potentials are expected to have only a smoothing effect on the resonance, since they mainly take into account only absorption effects. Therefore, existing phenomenological complex optical potentials cannot be used solely for the purpose of quantitatively reproducing cross sections in a study in which the main objective is to explore the fundamental qualitative characteristics of quasiparticle resonance.

For these reasons, in this paper we use the same model and parameters as in our previous papers [20,21] to investigate the qualitative characteristics of quasiparticle resonance in terms of vortices in the neutron current in *n-A* scattering, paying attention to the correspondence with our previous findings on the characteristics of quasiparticle resonance.

II. THEORETICAL AND CALCULATION BACKGROUND

In this paper, the HFB equation is solved by assuming spherical symmetry. We adopt the Woods-Saxon potential for the mean-field potential U and pair potential Δ with the same parameters as in Ref. [20] in order to clarify the correspondence between the results in this paper and our previous results [20,21,23]. (To distinguish our model from the self-consistent HFB equation based on the effective two-body nuclear force, we will hereafter refer to our model as WS-HFB in this paper.) The chemical potential $\lambda = -1$ MeV is adopted in order to set the neutron-rich target of the system.

The neutron current $\boldsymbol{j}$ of the *n-A* scattering system is defined as

$$\boldsymbol{j}(\boldsymbol{r}) = \operatorname{Im} \psi_1^{(+)*}(\boldsymbol{r}) \nabla \psi_1^{(+)}(\boldsymbol{r}) \tag{1}$$

by using the upper component of the WS-HFB scattering wave function $\psi_1^{(+)}(\boldsymbol{r})$. The vorticity $\boldsymbol{\omega}$ for the neutron current is defined by

$$\boldsymbol{\omega}(\boldsymbol{r}) = \nabla \times \boldsymbol{j}(\boldsymbol{r}) \tag{2}$$

$$= \frac{1}{i} \nabla \psi_1^{(+)*}(\boldsymbol{r}) \times \nabla \psi_1^{(+)}(\boldsymbol{r}) \tag{3}$$

The vorticity is a pseudovector which describes the strength and direction of the local spinning motion. The sign of the vorticity is defined as positive for counterclockwise spinning motion. The circulation Γ, which is defined by

$$\Gamma = \int_S d\boldsymbol{S} \cdot \boldsymbol{\omega}(\boldsymbol{r}), \tag{4}$$

is the total amount of vorticity in the area (S) enclosed by the closed path. By Stokes's theorem, the circulation can be rewritten as

$$\Gamma = \oint_C d\boldsymbol{l} \cdot \boldsymbol{j}(\boldsymbol{r}), \tag{5}$$

where C represents the closed path to give the area S.

In this paper, the direction of the incident neutron is taken as the z axis in the system of n-A scattering [i.e., $\boldsymbol{k}$ of $\exp(i\boldsymbol{k} \cdot \boldsymbol{r})$ is chosen as $\boldsymbol{k} = k\boldsymbol{e}_z$]. Since the scattering behavior of neutrons by spherical nuclei should be axially symmetric, we show the numerical results of the current ($\boldsymbol{j}$) and vorticity ($\boldsymbol{\omega}$) in the z-x plane, which is defined by setting $\varphi = 0$ in spherical coordinates. To correctly represent a plane wave $\exp(i\boldsymbol{k} \cdot \boldsymbol{r})$ up to 20 MeV in a region of 20 fm dynamic diameter, $l_{\max} = 20$ is adopted for the representation of the partial wave components.

In the z-x plane, the vorticity is represented as

$$\boldsymbol{\omega}(\boldsymbol{r}) = 2\boldsymbol{e}_y \, \mathrm{Im}[(\boldsymbol{e}_z \cdot \boldsymbol{\nabla}\psi_1^{(+)*}(\boldsymbol{r}))(\boldsymbol{e}_x \cdot \boldsymbol{\nabla}\psi_1^{(+)}(\boldsymbol{r}))]_{\varphi=0}, \quad (6)$$

where $\boldsymbol{e}_x$, $\boldsymbol{e}_y$, and $\boldsymbol{e}_z$ are the unit vectors for x, y, and z axes, respectively. Using the partial components of the scattering wave function, $\boldsymbol{e}_z \cdot \boldsymbol{\nabla}\psi_1^{(+)}(\boldsymbol{r})$ and $\boldsymbol{e}_x \cdot \boldsymbol{\nabla}\psi_1^{(+)}(\boldsymbol{r})$ are represented as

$$\boldsymbol{e}_z \cdot \boldsymbol{\nabla}\psi_1^{(+)}(\boldsymbol{r}) = \frac{1}{r}\sum_{lj}(i)^l \frac{2j+1}{2}\frac{\sqrt{4\pi}}{2l+1}$$
$$\times \left[\frac{l+1}{\sqrt{2l+3}}Y_{l+1,0}(\widehat{\boldsymbol{r}})\left(r - \frac{l+1}{r}\right) \right.$$
$$\left. + \frac{l}{\sqrt{2l-1}}Y_{l-1,0}(\widehat{\boldsymbol{r}})\left(r + \frac{l}{r}\right)\right]\psi_{1,lj}^{(+)}(r), \quad (7)$$

$$\boldsymbol{e}_x \cdot \boldsymbol{\nabla}\psi_1^{(+)}(\boldsymbol{r}) = \frac{1}{r}\sum_{lj}(i)^l \frac{2j+1}{2}\frac{\sqrt{4\pi}}{2l+1}$$
$$\times \left[-\sqrt{\frac{(l+1)(l+2)}{2l+3}}Y_{l+1,1}(\widehat{\boldsymbol{r}})\left(r - \frac{l+1}{r}\right) \right.$$
$$\left. + \sqrt{\frac{l(l-1)}{2l-1}}Y_{l-1,1}(\widehat{\boldsymbol{r}})\left(r + \frac{l}{r}\right)\right]\psi_{1,lj}^{(+)}(r). \quad (8)$$

Note that spin nonflip is supposed in these expressions. Although a spin-flip current can also be defined, the spin-flip component in n-A scattering is expected to be sensitive to dynamical effects such as PVC effects and spin-dependent terms in potentials and interactions, based on analyzing power and other results [25–27]. Therefore, we do not discuss the spin-flip current in this study, which uses a simple model.

We can obtain the Lippmann-Schwinger (LS) integral equation for the WS-HFB scattering wave function

$$\begin{pmatrix} \psi_1^{(+)}(\boldsymbol{r}) \\ \psi_2^{(+)}(\boldsymbol{r}) \end{pmatrix} = \begin{pmatrix} \psi_0^{(+)}(\boldsymbol{r}) \\ 0 \end{pmatrix}$$
$$+ \int d\boldsymbol{r}_1 \begin{pmatrix} G_0^{(+)}(\boldsymbol{r},\boldsymbol{r}_1;k_1(E)) & 0 \\ 0 & -G_0^{(+)}(\boldsymbol{r},\boldsymbol{r}_1;k_2(E)) \end{pmatrix}$$
$$\times \begin{pmatrix} 0 & \Delta(\boldsymbol{r}_1) \\ \Delta(\boldsymbol{r}_1) & 0 \end{pmatrix}\begin{pmatrix} \psi_1^{(+)}(\boldsymbol{r}_1) \\ \psi_2^{(+)}(\boldsymbol{r}_1) \end{pmatrix} \quad (9)$$

by applying the two-potential formula, where $\psi_0^{(+)}$ is the scattering wave function by the mean field potential U and

the Green's function which satisfies

$$\left(\frac{\hbar^2 k^2}{2m} + \frac{\hbar^2}{2m}\nabla^2 - U\right)G_0^{(+)}(\boldsymbol{r},\boldsymbol{r}';k) = \delta(\boldsymbol{r}-\boldsymbol{r}'), \quad (10)$$

$k_1(E)$ and $k_2(E)$ are defined by $k_1(E) = \sqrt{\frac{2m}{\hbar^2}(\lambda + E)}$ and $k_2(E) = \sqrt{\frac{2m}{\hbar^2}(\lambda - E)}$ as is introduced in Ref. [20].

The LS equation Eq. (9) can be expressed in the form of independent integral equations for the upper and lower components, respectively, using the WS-HFB Green's function $\mathcal{G}$ and the Dyson equation [Eq. (A1)].

The upper component can be expressed in two ways as

$$\psi_1^{(+)}(\boldsymbol{r}) = \begin{cases} \psi_0^{(+)}(\boldsymbol{r}) \\ + \iint d\boldsymbol{r}_1 d\boldsymbol{r}_2 \mathcal{G}_{11}^{(+)}(\boldsymbol{r},\boldsymbol{r}_1)\Sigma_0(\boldsymbol{r}_1,\boldsymbol{r}_2)\psi_0^{(+)}(\boldsymbol{r}_2), \\ \psi_0^{(+)}(\boldsymbol{r}) \\ + \iint d\boldsymbol{r}_1 d\boldsymbol{r}_2 G_0^{(+)}(\boldsymbol{r},\boldsymbol{r}_1;k_1)\Sigma(\boldsymbol{r}_1,\boldsymbol{r}_2)\psi_0^{(+)}(\boldsymbol{r}_2), \end{cases}$$
$$(11)$$

and the lower component is expressed in a form that is computed using the upper component as

$$\psi_2^{(+)}(\boldsymbol{r}) = -\int d\boldsymbol{r}_1 G_0^{(+)}(\boldsymbol{r},\boldsymbol{r}_1;k_2)\Delta(\boldsymbol{r}_1)\psi_1^{(+)}(\boldsymbol{r}_1), \quad (12)$$

with Σ_0 and Σ which are defined by

$$\Sigma_0(\boldsymbol{r},\boldsymbol{r}') = -\Delta(\boldsymbol{r})G_0^{(+)}(\boldsymbol{r},\boldsymbol{r}';k_2)\Delta(\boldsymbol{r}'), \quad (13)$$

$$\Sigma(\boldsymbol{r},\boldsymbol{r}') = \Delta(\boldsymbol{r})\mathcal{G}_{22}^{(+)}(\boldsymbol{r},\boldsymbol{r}')\Delta(\boldsymbol{r}'), \quad (14)$$

where $\mathcal{G}_{11}^{(+)}$ and $\mathcal{G}_{22}^{(+)}$ are the diagonal components of the WS-HFB Green's function which is expressed in 4×4 matrix form. It should be noticed that Eq. (13) is the first term to appear in the Dyson series expansion of Eq. (14) as $\Sigma = \Sigma_0 + \cdots$.

Of course, it is obvious that Σ_0 and Σ would behave as the nonlocal potential which originates from the pair correlation, and it is important to analyze the role of its nonlocality, but we will not discuss it yet in this paper.

In the HFB theory, it is known that quasiparticle states exist symmetrically in the positive and negative regions of quasiparticle energy. This is also true for the resonances (or more precisely, the poles of the S matrix corresponding to the resonances) [20]. There are two types of quasiparticle resonances, particle-type (p-type) and hole-type (h-type), both of which exist in both the positive and negative quasiparticle energy regions.

By performing the similar approximate calculations to derive the spectral representation of the WS-HFB Green function as shown in Ref. [23], it is possible to confirm that in the positive energy region ($E > 0$) a particle-type resonance behaves as a pole of $\mathcal{G}_{11}$ and a hole-type resonance behaves as a pole of $\mathcal{G}_{22}$, i.e.,

$$\langle p|\mathcal{G}_{11}|p\rangle \sim \frac{1}{E - E_{qp}^{(p)}}, \quad (15)$$

$$\langle h|\mathcal{G}_{22}|h\rangle \sim \frac{1}{E - E_{qp}^{(h)}}, \quad (16)$$

where $E_{qp}^{(p)}$ and $E_{qp}^{(h)}$ are the S-matrix poles for the particle-type and hole-type quasiparticle resonance energies which are given as complex numbers. The detail expressions of $E_{qp}^{(p)}$ and $E_{qp}^{(h)}$ are given in Refs. [20,21]. This is the origin of the metastable structure of the scattering wave function at the resonance energy.

By inserting Eq. (11) into Eqs. (1), we can divide the current j into three terms as

$$j = j_0 + j_{\text{int}} + \delta j \tag{17}$$

with

$$j_0 = \text{Im}\,\psi_0^{(+)*}\nabla\psi_0^{(+)}, \tag{18}$$

$$j_{\text{int}} = \text{Im}[\delta\psi^{(+)*}\nabla\psi_0^{(+)} + \psi_0^{(+)*}\nabla\delta\psi^{(+)}], \tag{19}$$

$$\delta j = \text{Im}\,\delta\psi^{(+)*}\nabla\delta\psi^{(+)}, \tag{20}$$

where $\delta\psi^{(+)}$ is the second term of Eq. (11) which includes the pair correlation, j_0 is the mean field (MF) current, j_{int} is the current which represents the interference between the MF scattering wave function $\psi_0^{(+)}$ and $\delta\psi^{(+)}$, and δj is the current formed by the scattered wave by the pair potential in the MF mean field ($\delta\psi^{(+)}$).

By using Eqs. (17), the vorticity is also divided into three terms as

$$\omega = \omega_0 + \omega_{\text{int}} + \delta\omega \tag{21}$$

with

$$\omega_0 = \nabla \times j_0 = 2e_y\,\text{Im}[(e_z \cdot \nabla\psi_0^{(+)*})(e_x \cdot \nabla\psi_0^{(+)})], \tag{22}$$

$$\omega_{\text{int}} = \nabla \times j_{\text{int}} = 2e_y\,\text{Im}[(e_z \cdot \nabla\delta\psi^{(+)*})(e_x \cdot \nabla\psi_0^{(+)}) - (e_x \cdot \nabla\delta\psi^{(+)*})(e_z \cdot \nabla\psi_0^{(+)})], \tag{23}$$

$$\delta\omega = \nabla \times \delta j = 2e_y\,\text{Im}[(e_z \cdot \nabla\delta\psi^{(+)*})(e_x \cdot \nabla\delta\psi^{(+)})]. \tag{24}$$

δj and $\delta\omega$ are expected to be smaller in absolute value (than j_{int} and ω_{int}) because they are quantities that give higher-order pairing contributions. However, the continuity equation for δj and j_{int} is given by

$$\nabla \cdot (j_{\text{int}} + \delta j) = 0 \tag{25}$$

since j and j_0 satisfy $\nabla \cdot j = 0$ and $\nabla \cdot j_0 = 0$, respectively. Equation (25) is shown to say $\nabla \cdot j_{\text{int}} \neq 0$ as long as $\delta j \neq 0$, $\nabla \cdot j_{\text{int}} \neq 0$ implies that j_{int} contains the "gushing" or "suctioning" motion of the current. If we define

$$j_{\text{pair}} = j_{\text{int}} + \delta j = j - j_0 \tag{26}$$

as the current representing the pairing contribution, j_{pair} does not include "gushing" or "suctioning" motion, i.e., $\nabla \cdot j_{\text{pair}} = 0$. The vorticity which corresponds to j_{pair} (ω_{pair}) is also defined as

$$\omega_{\text{pair}} = \nabla \times j_{\text{pair}} \tag{27}$$

$$= \omega_{\text{int}} + \delta\omega = \omega - \omega_0. \tag{28}$$

The approximated expression of ω_{pair} near the quasiparticle resonance energy can be represented as

$$\omega_{\text{pair}} \sim \begin{cases} \text{For particle-type quasiparticle resonance:} \\ \dfrac{(E - \text{Re}\,E_{qp}^{(p)})\,\text{Re}\langle p|\Sigma_0|\psi_0^{(+)}\rangle}{(E - \text{Re}\,E_{qp}^{(p)})^2 + (\text{Im}\,E_{qp}^{(p)})^2}2e_y\,\text{Im}[(e_z \cdot \nabla\phi_p^*)(e_x \cdot \nabla\psi_0^{(+)}) - (e_x \cdot \nabla\phi_p^*)(e_z \cdot \nabla\psi_0^{(+)})] \\ \quad\quad\quad\quad + (\text{other partial wave components of }\omega_{\text{int}}) + \delta\omega; \\ \text{For hole-type quasiparticle resonance:} \\ -\dfrac{(\text{Im}\,E_{qp}^{(h)})^2}{(E - \text{Re}\,E_{qp}^{(h)})^2 + (\text{Im}\,E_{qp}^{(h)})^2}\omega_0 + (\text{other partial wave components of }\omega_{\text{int}}) + \delta\omega. \end{cases} \tag{29}$$

(See the Appendix for a detailed derivation).

The first term of Eq. (29) can be obtained as a leading order term of ω_{int} by applying Eqs. (15) and (16) to Eq. (11). The contributions of other partial wave components of ω_{int} and $\delta\omega$ are expected to be very small compared to that of the first term. From Eq. (29), we can expect that the contribution of pairing to vorticity is quite different between p-type and h-type quasiparticle resonances. In the case of p-type, the positive and negative contributions of ω_{pair} are reversed depending on whether E is greater or less than $\text{Re}\,E_{qp}$.

Furthermore, ω_{pair} takes a maximum/minimum value at $E = \text{Re}\,E_{qp}^{(p)} \pm \text{Im}\,E_{qp}^{(p)}$. At these energies, ω_{pair} can be expressed as

$$\omega_{\text{pair}}(E = \text{Re}\,E_{qp}^{(p)} \pm \text{Im}\,E_{qp}^{(p)}) \sim \pm\frac{\text{Re}\langle p|\Sigma_0|\psi_0^{(+)}\rangle}{2(\text{Im}\,E_{qp}^{(p)})}2e_y\,\text{Im}[(e_z \cdot \nabla\phi_p^*)(e_x \cdot \nabla\psi_0^{(+)}) - (e_x \cdot \nabla\phi_p^*)(e_z \cdot \nabla\psi_0^{(+)})]$$

$$+ (\text{other partial wave components of }\omega_{\text{int}}) + \delta\omega. \tag{30}$$
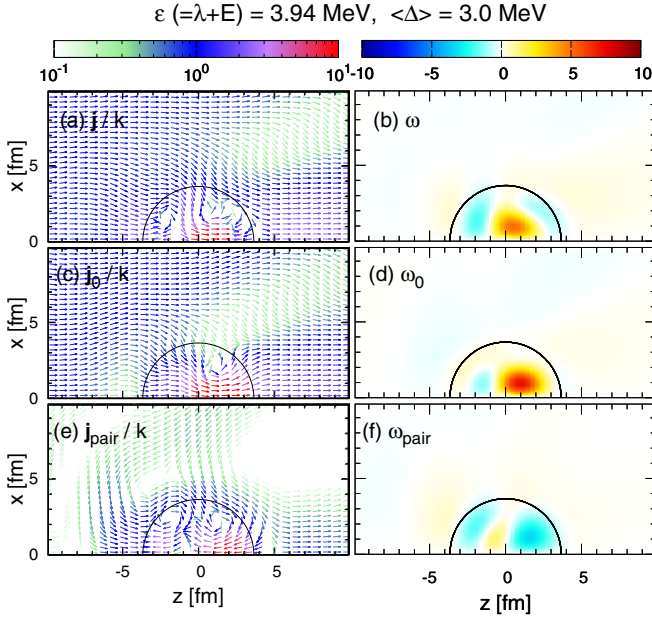
FIG. 1. The neutron currents (a) $\boldsymbol{j}$, (c) $\boldsymbol{j}_0$, and (e) $\boldsymbol{j}_{\mathrm{pair}}$ at $\epsilon = 3.94$ MeV (an energy corresponding to the h-type $d_{3/2}$ resonance) with $\lambda = -1.0$ MeV and $\langle\Delta\rangle = 3.0$ MeV. The panels (b), (d), and (f) are the vortices corresponding to the currents (a), (c), and (e), respectively. The arrows representing current are the same length. The strength (absolute value) of the current, which is normalized by $k(= \sqrt{\frac{2m}{\hbar^2}(\lambda + E)})$ (the absolute value of the plane wave) is represented by color. The unit of the vorticity is fm^{-2}. The black solid semicircle shows the size of the target nucleus given by $r_0 A^{\frac{1}{3}} = 3.66$ fm.

FIG. 2. The contour plot of Γ as a function of ϵ and $\langle\Delta\rangle$. The dotted curves represent the real part of the S-matrix poles for the quasiparticle resonances which were shown in Ref. [20].

Since Im $E_{qp}^{(p)}$ expresses the half-width of resonance, the maximum value of $\boldsymbol{\omega}_{\mathrm{pair}}$ is inversely proportional to the width of the resonance (i.e., proportional to the lifetime of the resonance). This is the very result which we expected in the introduction of this paper.

In the case of h-type, if we can ignore all but the first term (leading term), the pairing effect leads to zero vorticity, i.e., the vortices disappear at $E = \mathrm{Re}\, E_{qp}^{(h)}$, because $\boldsymbol{\omega}_{\mathrm{pair}}$ becomes

$$\boldsymbol{\omega}_{\mathrm{pair}}(E = \mathrm{Re}\, E_{qp}^{(h)})$$
$$\sim -\boldsymbol{\omega}_0 + (\text{other partial wave components of } \boldsymbol{\omega}_{\mathrm{int}}) + \delta\boldsymbol{\omega}. \tag{31}$$

The pair correlation for the h-type resonance has the effect of vanishing vortices created by MF potential scattering and, contrary to our expectation, has no relation to the width of the resonance (the lifetime of the resonance), which is quite different from that of p-type resonances.

However, in the definition of a vortex, each partial wave component is complexly coupled, so it is impossible to perform a numerical calculation that extracts only the leading term. In particular, it is expected that as the pair-correlation becomes stronger, the pair-correlation effect on other partial wave components that are not in resonance will become non-negligible.

As is shown in [20,21], the width of the quasiparticle resonance increases as the pair-correlations become stronger,
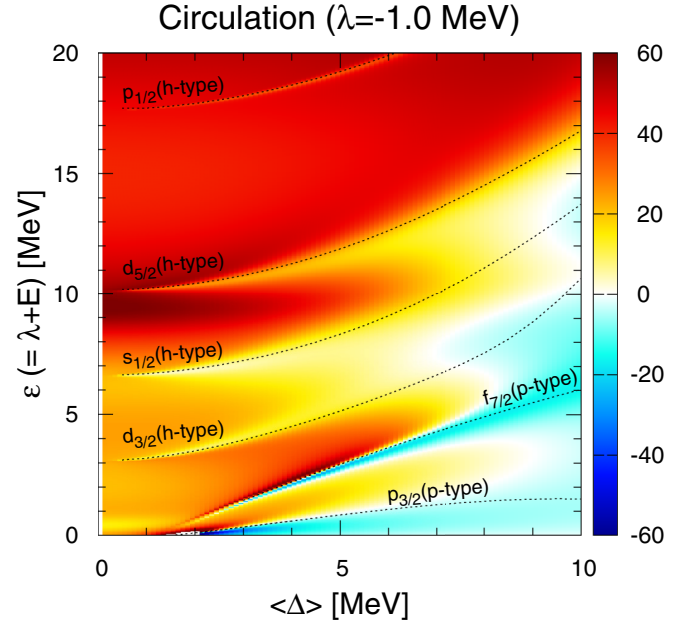
but, within the range of realistic pair-correlation strengths, the width of the quasiparticle resonance does not change very much. In particular, the change is negligible for p-type resonances. Therefore, it is difficult to directly show properties such as the relationship between vortex and resonance width as a result of numerical calculations.

Fortunately, however, Eq. (29) also shows that the qualitative properties of vortices themselves are completely different between p-type and h-type resonances, so if we can actually confirm that the qualitative properties of vorticity are completely different between p-type and h-type resonances by analyzing the results of numerical calculations and then confirm that they are consistent with Eq. (29), we can confirm the relationship between the vortex and resonance width that the main terms indicate, albeit indirectly.

III. NUMERICAL RESULTS

In Fig. 1, the neutron currents ($\boldsymbol{j}$, $\boldsymbol{j}_0$, and $\boldsymbol{j}_{\mathrm{pair}}$) and the vorticities ($\boldsymbol{\omega}$, $\boldsymbol{\omega}_0$, and $\boldsymbol{\omega}_{\mathrm{pair}}$) at the energy corresponding to the h-type $d_{3/2}$ resonance are shown in the left and right panels, respectively.

As given in Eqs. (4) and (5), the circulations (Γ, Γ_0 and Γ_{pair}) are calculated by the area integrations of $\boldsymbol{\omega}$, $\boldsymbol{\omega}_0$, and $\boldsymbol{\omega}_{\mathrm{pair}}$ or line integrations of $\boldsymbol{j}$, $\boldsymbol{j}_0$, and $\boldsymbol{j}_{\mathrm{pair}}$. Since the current is symmetric about the z axis, the region of the upper half of the z-x plane $0 \leqslant x \leqslant 10$ fm, $-10 \leqslant z \leqslant 10$ fm (the area showing current and vorticity in Fig. 1) is adopted as the integration area for the calculation of the circulation.

In Fig. 2, the contour plot of the circulation Γ is shown as a function of the energy ϵ and mean pairing gap $\langle\Delta\rangle$. The black dotted curves are the real parts of the S-matrix poles for the quasiparticle resonances shown in Figs. 6 and 7 in
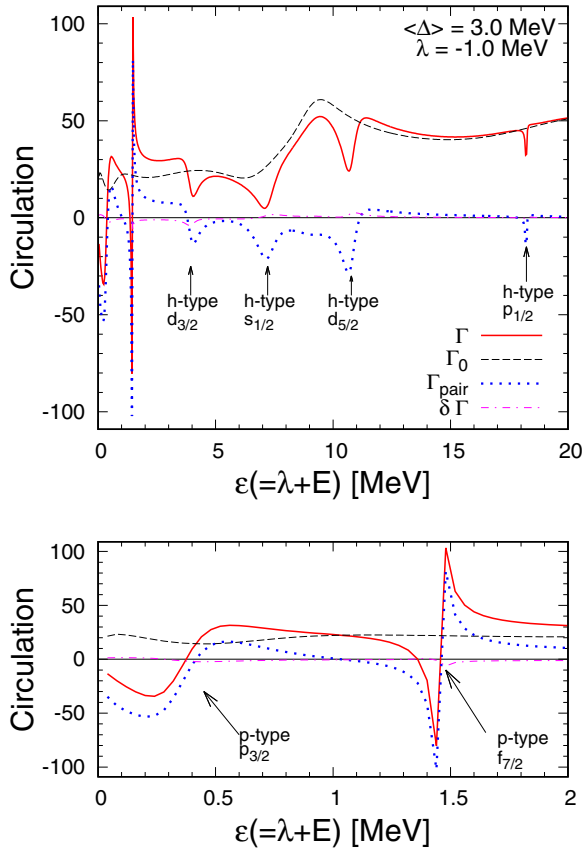
FIG. 4. The current $\boldsymbol{j}_{\mathrm{pair}}$ and vorticity $\boldsymbol{\omega}_{\mathrm{pair}}$ at $\epsilon = 1.45 - 1.16 \times 10^{-2}$, 1.45, and $1.45 + 1.16 \times 10^{-2}$ MeV; $\epsilon = 1.45$ MeV is the energy at which Γ_{pair} becomes zero (found near the real part of the S-matrix pole of the p-type $f_{7/2}$ resonance), and $\pm 1.16 \times 10^{-2}$ MeV is the imaginary part of the S-matrix pole (half-width of the resonance).

FIG. 3. The circulation obtained by integrating the area of the region $0 \leqslant x \leqslant 10$ fm, $-10 \leqslant z \leqslant 10$ fm (the area as shown in Fig. 1), or by line integrating this region in a counterclockwise direction. Γ (red solid), Γ_0 (black dash), Γ_{pair} (blue dot), and $\delta\Gamma$ (purple dot-dash) are the circulations which are corresponding to $\boldsymbol{\omega}$, $\boldsymbol{\omega}_0$, $\boldsymbol{\omega}_{\mathrm{pair}}$, and $\delta\boldsymbol{\omega}$, respectively. The lower panel shows an enlargement of the region $0 \leqslant \epsilon \leqslant 2$ MeV to make it easier to see the circulation for the p-type resonances.

Ref. [21]. The curvilinear pattern in the contour plot of the circulation coincides with the curve of the real part of the pole of the S matrix of the quasiparticle resonance, indicating that the circulation of the incident neutron flux in n-A scattering is greatly affected by the pairing effect at the quasiparticle resonance energy.

In Fig. 3, Γ, Γ_0, and Γ_{pair} calculated with $\langle\Delta\rangle = 3.0$ MeV are plotted as a function of the energy ϵ, and $\delta\Gamma$ which is obtained from $\delta\boldsymbol{\omega}$ (or $\delta\boldsymbol{j}$) is also shown in order to see the contribution. In the previous section, we expected that $\delta\boldsymbol{\omega}$ would be negligible as a contribution to $\boldsymbol{\omega}_{\mathrm{pair}}$ because it provides a higher-order contribution of the pairing. The correctness of our expectation is confirmed by the fact that $\delta\Gamma$, shown as a purple dotted curve in Fig. 3, is actually negligibly small. The characteristics of the p-type and h-type quasiparticle resonances for $\boldsymbol{\omega}_{\mathrm{pair}}$ shown in Eq. (29) are clearly expressed in the energy dependence of the circulation Γ_{pair} in Fig. 3.

As shown in Eq. (29), the Γ_{pair} calculated from $\boldsymbol{\omega}_{\mathrm{pair}}$ takes the form of a Lorentz distribution and acts to reduce Γ near the h-type quasiparticle resonance. From the current point of
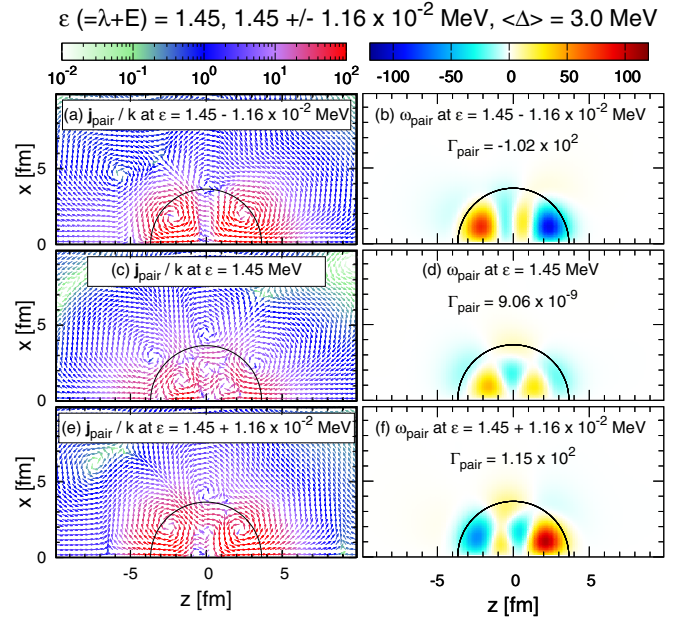
view, it can be seen from Fig. 1 that the pairing effect, $\boldsymbol{j}_{\mathrm{pair}}$, occurs in the direction of counteracting the current $\boldsymbol{j}_0$ in the nucleus, and acts to reduce the vorticity $\boldsymbol{\omega}$. In the case of the h-type quasiparticle resonances, the pairing correlation works to create a flow along the surface while preventing the incident neutron current from entering the target nucleus.

As indicated in Eq. (29), the effect of pairing on p-type quasiparticle resonances is quite different. In the case of p-type quasiparticle resonance, the pairing acts to reduce the circulation Γ on the lower side of the resonance energy (the real part of the S-matrix pole), but in contrast it acts to increase the circulation Γ in the energy region higher than the resonance energy. Figure 4 shows the currents $\boldsymbol{j}_{\mathrm{pair}}$ and their vorticities $\boldsymbol{\omega}_{\mathrm{pair}}$ for the p-type quasiparticle resonance at $f_{7/2}$. Panels (a), (c), and (e) show the currents at $\epsilon = 1.45 - 1.16 \times 10^{-2}$, 1.45, and $1.45 + 1.16 \times 10^{-2}$ MeV, respectively, and panels (b), (d), and (f) show the corresponding vorticities, where 1.45 MeV is the quasiparticle energy (the real part of the S-matrix pole of $f_{7/2}$), and 1.16×10^{-2} MeV is the half-width of the resonance (the imaginary part of the S-matrix pole).

In Fig. 4, we can see the obvious vortex that the current creates. In panel (a), there is a clockwise vortex in the $z > 0$ region and a counterclockwise vortex in the $z < 0$ region. In panel (e), these vortices are reversed. Since the vortices in the $z > 0$ region are stronger in both cases, the vorticity is negative in panel (a) and positive in panel (e). In panel (c), the weak vortices are symmetrically located inside and outside the nucleus, so that the overall vorticity is almost zero. It should
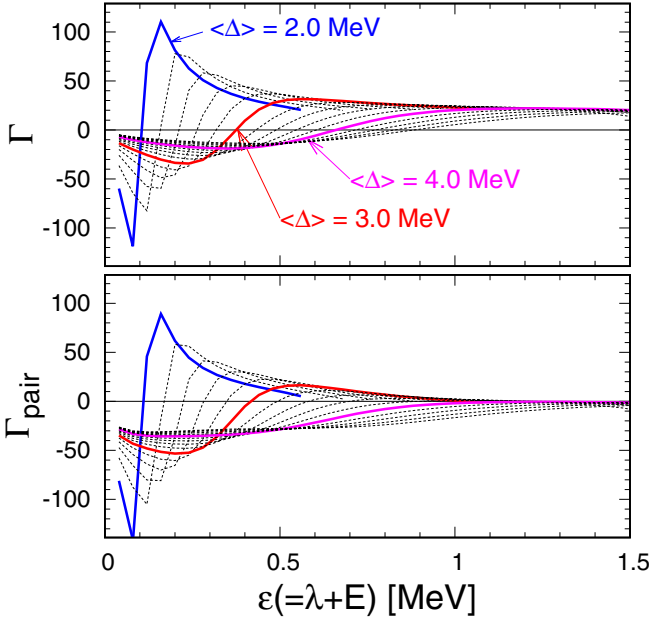
FIG. 5. The pairing dependence of the circulations Γ and Γ_{pair} around the energy region for the p-type $p_{3/2}$ resonance. The solid blue, red, and purple curves represent the circulation with $\langle\Delta\rangle = 2.0$, 3.0, and 4.0 MeV, respectively. The dotted curves show the circulation calculated every 0.2 MeV.

be noted that, since the current is symmetric about the z axis, the vortex is torus shaped (like a donut about the z axis).

As shown in Ref. [21], the $f_{7/2}$ p-type quasiparticle resonance is a resonant state that appears at energies lower than the centrifugal barrier, and the behavior of the $f_{7/2}$ partial wave component of the scattering WS-HFB wave function is more like a bound state than a metastable state. Since j_{int} is dominant in j_{pair} defined in Eq. (26), where j_{int} is defined in Eq. (19), the vortices arise from the interference between the partial wave component of the WS-HFB wave function for $f_{7/2}$ and the MF scattering wave function.

By carefully observing the current flow in Fig. 4, we can see that in panel (a) the current is only allowed to enter the nucleus from the front ($z > 0$ region, $\theta \approx 0$), while in panel (e) the current is allowed to enter from the back region ($z < 0$ region). Qualitatively, this is a common property of p-type quasiparticle resonances, although the angle at which the current is allowed to flow into the nucleus from the back region and the formation of vortices are different for $p_{3/2}$ and $f_{7/2}$.

In Ref. [21], we showed that when the independent K-matrix pole is located near the quasiparticle resonance, the correlation between the K-matrix pole of the quasiparticle resonance and the independent K-matrix pole causes the K-matrix pole to disappear when the pairing gap $\langle\Delta\rangle$ becomes larger than the critical gap $\langle\Delta\rangle_c$. We also showed that the critical gap of the p-type $p_{3/2}$ is $\langle\Delta\rangle_c = 4.08$ MeV.

Figure 5 shows how the circulations Γ and Γ_{pair} change when the pairing gap is varied around the energy region of the p-type $p_{3/2}$ quasiparticle resonance. From the analysis of this figure, we found that the energy for which $\Gamma = 0$ is found

almost at the same energy of the real part of the S-matrix pole, and the energy for which $\Gamma_{\text{pair}} = 0$ is found almost at the same energy as the K-matrix pole when $\langle\Delta\rangle < \langle\Delta\rangle_c$, but no longer exists when $\langle\Delta\rangle > \langle\Delta\rangle_c$.

IV. SUMMARY

In this paper, we analyze the effect of pairing on incident neutron current in n-A scattering described within the framework of HFB theory. For this purpose, the current was defined using the WS-HFB scattering wave function and its numerical calculation was performed. To analyze the effect of pairing, the current was decomposed into a MF part and a pairing part, and the corresponding vorticity and circulation were also calculated and analyzed.

It was found that the pairing effects on current, vorticity, and circulation are quite different between p-type and h-type quasiparticle resonances. In the case of the h-type quasiparticle resonances, the pairing has the effect of preventing the neutron current from flowing into the nucleus, which reduces vorticity and circulation. In the case of the p-type quasiparticle resonance, the pairing acts to prevent neutron current from entering the nucleus in the energy region below the resonance energy, while the pairing acts to allow neutron current from the backward region to enter in the energy region above the resonance energy. Vortices appear due to the presence of metastable structures of a certain partial wave component, but the direction of the vortices is reversed below and above the resonance energy. These features are consistent with the results of Eq. (29), which shows how the S-matrix poles of p-type and h-type quasiparticle resonances contribute to the vorticity.

As a characteristic of quasiparticle resonance indicated by Eq. (29), it can be said that, for p-type resonance, vorticity and resonance width are inversely proportional, i.e., vorticity and resonance lifetime are proportional [Eq. (30)]. However, in contrast, in h-type resonances, the vortex created by MF scattering is canceled out by the pair correlation effect, which is not related to the resonance width [Eq. (31)]. We also found that the effect of the disappearance of the K-matrix pole due to the correlation between the independent K-matrix pole near the quasiparticle resonance and the K matrix of the quasiparticle resonance (which has been discussed in Ref. [21]) appears in the form of the disappearance of the energy which satisfies $\Gamma_{\text{pair}} = 0$.

In order to discuss the dynamic features and properties of vortices in quantum systems in more detail, it is necessary to derive the fluid equation based on the Schrödinger equation (including the HFB equation, etc.) and discuss it in terms of the quantum pressure term that will appear in the fluid equation, touching on the violation of Kelvin's circulation theorem and the hydrodynamic conservation law. The development of a self-consistent cQVC method based on the effective two-body nuclear force and the extension of the Jost function method to the cQVC method to calculate the width of resonances based on the cQVC method would also be important issues for a more realistic and quantitative analysis and a deeper exploration of vortex properties as described above.

However, we leave them for future work without touching on them in this paper.

APPENDIX: DERIVATION OF EQ. (29)

The WS-HFB Green's function satisfies the following Dyson equation:

$$\mathcal{G} = \mathcal{G}_0 + \int dr \mathcal{G}_0 V_{\text{pair}} \mathcal{G} \tag{A1}$$

with

$$\mathcal{G} = \begin{pmatrix} \mathcal{G}_{11} & \mathcal{G}_{12} \\ \mathcal{G}_{21} & \mathcal{G}_{22} \end{pmatrix}, \tag{A2}$$

$$\mathcal{G}_0 = \begin{pmatrix} G_0(k_1) & 0 \\ 0 & -G_0(k_2) \end{pmatrix}, \tag{A3}$$

and

$$V_{\text{pair}} = \begin{pmatrix} 0 & \Delta \\ \Delta & 0 \end{pmatrix}. \tag{A4}$$

By using Eq. (13), this Dyson equation (A1) can be rewritten as

$$\mathcal{G}_{11} = G_0(k_1) + G_0(k_1)\Sigma_0 \mathcal{G}_{11}. \tag{A5}$$

$$\mathcal{G}_{22} = -G_0(k_2) - G_0(k_2)\Delta G_0(k_1)\Delta \mathcal{G}_{22}. \tag{A6}$$

By inserting Eq. (A6) into Eq. (14), we can obtain

$$\Sigma = \Sigma_0 + \Sigma_0 G_0(k_1)\Sigma. \tag{A7}$$

By applying Eq. (A5) or (A7) to the series expansion of Eq. (9), we can obtain Eq. (11).

Since $\delta\psi^{(+)} = \psi_1^{(+)} - \psi_0^{(+)}$ and the poles of the particle- and hole-type resonances are given as the poles of $\mathcal{G}_{11}$ and $\mathcal{G}_{22}$ as shown by Eqs. (15) and (16) respectively, we can obtain the approximated expression for $\delta\psi^{(+)}$ by using Eq. (11) as

$$\delta\psi^{(+)} = \psi^{(+)} - \psi_0^{(+)} \tag{A8}$$

$$= \begin{cases} \mathcal{G}_{11}\Sigma_0\psi_0^{(+)} \sim \psi_{qp}\frac{\langle\psi_{qp}|\Sigma_0|\psi_0^{(+)}\rangle}{E - E_{qp}^{(p)}}, \\ G_0\Sigma\psi_0^{(+)} \sim -i\frac{2mk_1}{\hbar^2}\psi_0(k_1)\frac{|\langle\psi_0^{(+)}(k_1)|\Delta|\psi_{qp}\rangle|^2}{E - E_{qp}^{(h)}} \end{cases} \tag{A9}$$

for the particle- and hole-type resonances, respectively.

By inserting Eq. (A9) into Eq. (23) and using Eq. (28), Eq. (29) can be derived.

[1] R. P. Feynmann, Prog. Low. Temp. Phys. **1**, 17 (1955).
[2] A. A. Abrikosov, Sov. Phys. JETP **5**, 1174 (1957).
[3] C. J. Kennedy, W. C. Burton *et al.*, Nat. Phys. **11**, 859 (2015).
[4] Y.-J. Lin, R. L. Compton, K. Jiménez-García *et al.*, Nature (London) **462**, 628 (2009).
[5] S. Stringari, Phys. Lett. A **347**, 150 (2005).
[6] M. M. Salomaa and G. E. Volovik, Rev. Mod. Phys. **59**, 533 (1987).
[7] M. R. Matthews, B. P. Anderson, P. C. Haljan, D. S. Hall, C. E. Wieman, and E. A. Cornell, Phys. Rev. Lett. **83**, 2498 (1999).
[8] I. N. Mikhailov, P. Quentin, and D. Samsoen, Nucl. Phys. A **627**, 259 (1997).
[9] I. N. Mikhailov and P. Quentin, Phys. Rev. Lett. **74**, 3336 (1995).
[10] D. M. Brink and R. A. Broglia, *Nuclear Superfluidity: Pairing in Finite Systems* (Cambridge University Press, Cambridge, 2005).
[11] O. Elgaroy and F. V. De Blasio, Astron. Astrophys. **370**, 939 (2001).
[12] J. A. Sauls, Superfluidity in the interiors of neutron stars, *Timing Neutron Stars* (Springer, Dordrecht, 1989), pp. 457–490.
[13] G. Baym, C. Pethick, and D. Pines, Nature (London) **224**, 673 (1969).
[14] D. Langlois, D. M. Sedrakian, and B. Carter, Mon. Not. R. Astron. Soc. **297**, 1189 (1998).
[15] S. F. Semenko, Sov. J. Nucl. Phys. **34**, 356 (1981).

[16] N. Ryezayeva, T. Hartmann, Y. Kalmykov, H. Lenske, P. von Neumann-Cosel, V. Y. Ponomarev, A. Richter, A. Shevchenko, S. Volz, and J. Wambach, Phys. Rev. Lett. **89**, 272502 (2002).
[17] K. Sasaki, N. Suzuki, and H. Saito, Phys. Rev. Lett. **104**, 150404 (2010).
[18] J. Dobaczewski, W. Nazarewicz, T. R. Werner, J. F. Berger, C. R. Chinn, and J. Decharge, Phys. Rev. C **53**, 2809 (1996).
[19] Y. Kobayashi and M. Matsuo, Prog. Theor. Exp. Phys. **2016** 013D01 (2016).
[20] K. Mizuyama, N. N. Le, T. D. Thuy, and T. V. Nhan Hao, Phys. Rev. C **99**, 054607 (2019).
[21] K. Mizuyama, H. Cong Quang, T. Dieu Thuy, and T. V. Nhan Hao, Phys. Rev. C **104**, 034606 (2021).
[22] G. G. Dussel, R. Id Betanb, R. J. Liotta, and T. Vertse, Nucl. Phys. A **789**, 182 (2007).
[23] K. Mizuyama, N. N. Le, and T. V. Nhan Hao, Phys. Rev. C **101**, 034601 (2020).
[24] K. Mizuyama and K. Ogata, Phys. Rev. C **86**, 041603(R) (2012).
[25] G. Blanchon, M. Dupuis, H. F. Arellano, and N. Vinh Mau, Phys. Rev. C **91**, 014612 (2015).
[26] T. V. Nhan Hao, B. M. Loc, and N. H. Phuc, Phys. Rev. C **92**, 014605 (2015).
[27] N. Hoang Tung, D. Quang Tam, V. N. T. Pham, C. Lam Truong, and T. V. Nhan Hao, Phys. Rev. C **102**, 034608 (2020).